1P3-4

Proceedings of Symposium on Ultrasonic Electronics, Vol. 37 (2016)
16-18 November, 2016

High Electromechanical Coupling of Sezawa Mode SAW Using a Polarization-Inverted ScAlN Film/High-Velocity Substrate Structure

極性反転 ScAlN 膜/高音速基板構造における
セザワ波の高い電気機械結合係数

Shinji Takayanagi[1‡] and Takahiko Yanagitani[2]
([1]Nagoya Inst. Tech.; [2]Waseda Univ.)
高柳 真司 [1‡], 柳谷 隆彦 [2]（[1]名工大, [2]早稲田大）

1. Introduction

ScAlN films are well researched for acoustic devices with high electromechanical coupling[1)]. In addition, ScAlN film on a high acoustic wave velocity substrate (e.g. diamond, SiC) realize the SAW devices operating in GHz range[2)].

Hexagonal crystals including ScAlN have piezoelectric polarization in the c-axis direction. The c-axis oriented film can be classified as either (0001) polarity or (000-1) polarity. Piezoelectric constants of (0001) oriented film are opposite in sign to those of (000-1) oriented film. The control of the polarity make it possible to obtain high-performance FBARs. For example, a polarization-inverted multilayer FBAR excites high overtone mode resonance, enabling high frequency or high power operation.

In previous study, we fabricated BAW resonators with the polarization-inverted ScAlN bilayer on a silica glass substrate[3)]. A BAW resonator with usual c-axis oriented film excites fundamental mode acoustic resonances. On the other hand, the BAW resonators with the polarization-inverted bilayer excites second overtone mode acoustic resonance. The strain of (0001) layer is generated in opposite direction of that of (000-1) layer by applying electric field to polarization-inverted bilayer. Second mode resonance is then exited. We consider that the excitation of second mode Rayleigh SAW (Sezawa mode SAW) can be excited with high electromechanical coupling coefficient K^2 using the polarization-inverted bilayer.

In this study, the SAW propagation properties of polarization-inverted (000-1)/(0001) $Sc_{0.4}Al_{0.6}N$ bilayer/diamond substrate were theoretically analyzed.

2. Calculation method

Figure 1 shows twelve configurations of boundary conditions considered in polarization-inverted film/substrate structure. These configurations correspond to the possible placements of metal shorting planes or IDT. The thickness of polarization-inverted bilayer was defined as shown in **Fig. 2**. H is the whole thickness of polarization-inverted bilayer, and r_H is the ratio of bottom film thickness to H. The propagation characteristics of SAWs calculated using a method proposed by Campbell and Jones[4)].

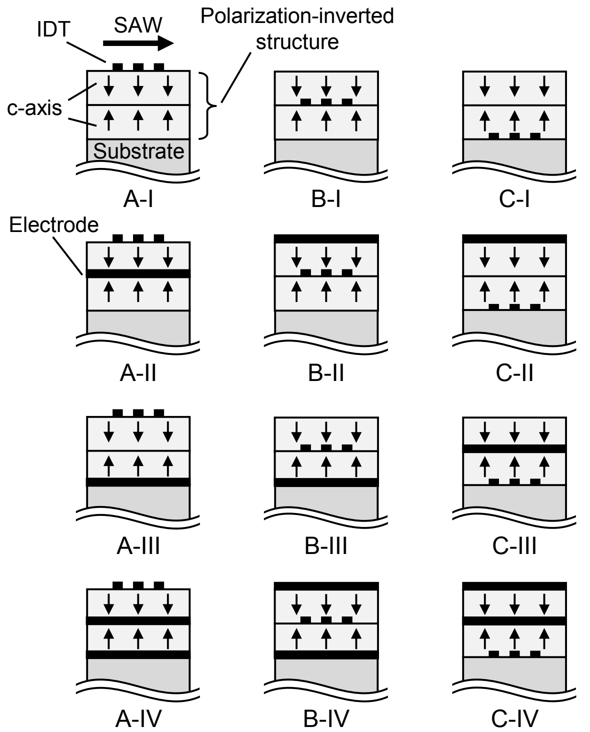

Fig. 1 Twelve configurations of boundary conditions used in the calculations for SAW propagation properties.

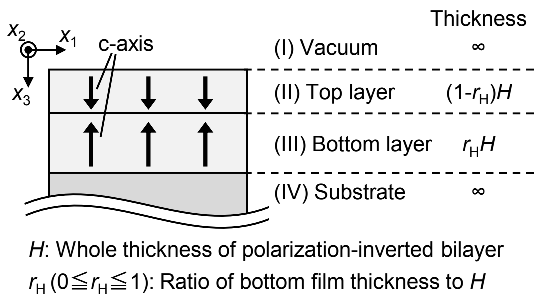

Fig. 2 Thickness definitions of each layer. r_H and H/λ were changed in the calculations.

E-mail : takayanagi.shinji@nitech.ac.jp

3. SAW propagation properties

Fig. 3 shows contour plots of the culculated K^2 values of the Sezawa mode SAW as functions of normalized film thickness H/λ and r_H in the polarization-inverted $Sc_{0.4}Al_{0.6}N$ bilayer/diamond. Elastic and piezoelectric constant tensors of ScAlN calculated by Caro *et al.*[5] were used in the K^2 calculation. The summary of maximum K^2 values of the first Rayleigh mode and Sezawa mode in each structure is shown in **Table I**. The maximum K^2 value was 15.4% in Sezawa mode of configuration B-IV at $H/\lambda = 0.18$ and $r_H = 0.46$. r_H of 0.46 means that top layer thickness is almost same as bottom layer thickness. Phase velocity V on an electrically free surface is 10,250 m/s. K^2 values in usual c-axis oriented $Sc_{0.4}Al_{0.6}N$ film/diamond were also calculated for comparison. The maximum K^2 was less than 12.0%. Therefore, high K^2 values were obtained in Sezawa mode propagating at the boundary of polarization-inverted ScAlN bilayer. In addition, displacements u_1 and u_3 of Sezawa mode SAW in depth (x_3) direction at K^2 = 15.4% in B-IV structure were investigated. The displacement u_1 is almost symmetric with respect to the boundary between top and bottom layer.

The propagation characteristics of SAWs in the polarization-inverted $Sc_{0.4}Al_{0.6}N$/6H-SiC were also analyzed. The maximum K^2 value was found to be 10.1% in Sezawa mode of configuration B-IV at $H/\lambda = 0.32$ and $r_H = 0.38$. It increased 1.5 times compared with the K^2 value in usual c-axis oriented $Sc_{0.4}Al_{0.6}N$/6H-SiC structure (6.6%).

4. Conclusions

In this study, the theoretically analyzed the K^2 values in the polarization-inverted $Sc_{0.4}Al_{0.6}N$ bilayer/diamond. High K^2 value (15.4%) was obtained in the Sezawa mode propagating at the boundary of polarization-inverted bilayer. The Sezawa mode SAW in the polarization-inverted ScAlN bilayer/ high-velocity substrate is a promising candidate for SAW devices.

References

1. T. Yanagitani, K. Arakawa, K. Kano, A. Teshigahara, and M. Akiyama: Proc. IEEE Int. Ultrasonics Symp., 2010, p. 2095.
2. K. Hashimoto, S. Sato, A. Teshigahara, T. Nakahara, and K. Kano: IEEE Trans. Ultrason. Ferroelectr. Freq. Control **60** (2013) 637.
3. M. Suzuki, T. Yanagitani, and H. Odagawa: Appl. Phys. Lett. **104** (2014) 172905.
4. J. J. Campbell and W. R. Jones: IEEE Trans. Sonics Ultrason. **15** (1968) 209.
5. M. A. Caro, S. Zhang, M. Ylilammi, T. Riekkinen, M. A. Moram, O. Lopez-Acevedo, J. Molarius, and T. Laurila: J. Phys. Condens. Matter **27** (2015) 245901.

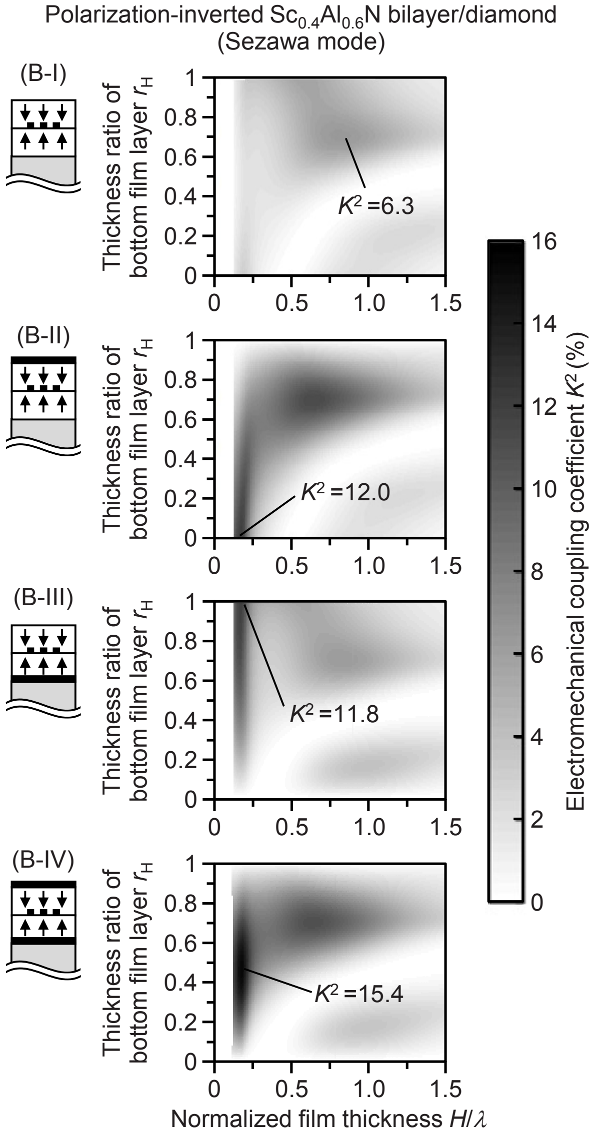

Fig. 3 Contour plots of K^2 of Sezawa mode SAW as functions of H/λ and r_H in polarization inverted $Sc_{0.4}Al_{0.6}N$ bilayer/diamond.

Table I Maximum K^2 values in each structure

	Polarization-inverted $Sc_{0.4}Al_{0.6}N$ bilayer/diamond					
	1st Rayleigh mode			Sezawa mode		
Structure	r_H	H/λ	K^2 (%)	r_H	H/λ	K^2 (%)
A-I	0.83	0.43	2.6	0.39	0.57	6.9
A-II	0	0.26	4.2	0.04	0.18	11.8
A-III	0.84	0.27	6.1	0	0.18	11.8
A-IV	0	0.26	4.2	0.02	0.18	11.8
B-I	0	0.37	6.0	0.70	0.82	6.3
B-II	0	0.30	8.3	0	0.17	12.0
B-III	0.37	0.35	10.7	0.95	0.17	11.8
B-IV	0.32	0.33	12.2	0.46	0.18	15.4
C-I	0.87	0.37	6.1	0.36	0.73	4.0
C-II	0.85	0.30	9.2	1	0.17	12.0
C-III	0.64	0.30	11.0	0.91	0.17	12.2
C-IV	0.64	0.30	11.0	0.90	0.17	12.2